

Aspect angle for interstellar magnetic field in SN 1006

O. Petruk,^{1,2*} G. Dubner,³ G. Castelletti,³ F. Bocchino,^{4,5} D. Iakubovskiy,⁶
M. G. F. Kirsch,⁷ M. Miceli,^{4,5} S. Orlando^{4,5} and I. Telezhinsky⁸

¹*Institute for Applied Problems in Mechanics and Mathematics, Naukova St 3-b, 79060 Lviv, Ukraine*

²*Astronomical Observatory, National University, Kyryla and Methodia St 8, 79008 Lviv, Ukraine*

³*Instituto de Astronomía y Física del Espacio (IAFE), CC 67, Suc. 28, 1428 Buenos Aires, Argentina*

⁴*INAF - Osservatorio Astronomico di Palermo, Piazza del Parlamento 1, 90134 Palermo, Italy*

⁵*Consorzio COMETA, Via S. Sofia 64, 95123 Catania, Italy*

⁶*Bogolyubov Institute for Theoretical Physics, Metrologichna St 14-b 03780 Kiev, Ukraine*

⁷*European Space Agency (ESA), European Space Operations Centre (ESOC), Robert-Bosch-Str. 5, D-64293 Darmstadt, Germany*

⁸*Astronomical Observatory, Kiev National Taras Shevchenko University, Observatorna St 3, 04053 Kiev, Ukraine*

Accepted 2008 November 14. Received 2008 November 13; in original form 2008 June 3

ABSTRACT

A number of important processes taking place around strong shocks in supernova remnants (SNRs) depend on the shock obliquity. The measured synchrotron flux is a function of the aspect angle between interstellar magnetic field (ISMF) and the line of sight. Thus, a model of non-thermal emission from SNRs should account for the orientation of the ambient magnetic field. We develop a new method for the estimation of the aspect angle, based on the comparison between observed and synthesized radio maps of SNRs, making different assumptions about the dependence of electron injection efficiency on the shock obliquity. The method uses the azimuthal profile of radio surface brightness as a probe for orientation of ambient magnetic field because it is almost insensitive to the downstream distribution of magnetic field and emitting electrons. We apply our method to a new radio image of SN 1006 produced on the basis of archival Very Large Array and Parkes data. The image recovers emission from all spatial structures with angular scales from a few arcsec to 15 arcmin. We explore different models of injection efficiency and find the following best-fitting values for the aspect angle of SN 1006: $\phi_o = 70^\circ \pm 4.2^\circ$ if the injection is isotropic, $\phi_o = 64^\circ \pm 2.8^\circ$ for quasi-perpendicular injection (SNR has an equatorial belt in both cases) and $\phi_o = 11^\circ \pm 0.8^\circ$ for quasi-parallel injection (polar-cap model of SNR). In the last case, SN 1006 is expected to have a centrally peaked morphology contrary to what is observed. Therefore, our analysis provides some indication against the quasi-parallel injection model.

Key words: acceleration of particles – radiation mechanisms: non-thermal – shock waves – cosmic rays – ISM: individual: SN 1006 – supernova remnants.

1 INTRODUCTION

Non-thermal emission of supernova remnants (SNRs) is intensively studied. It carries out important information about physics of strong shocks, kinetics of cosmic rays and magnetic field (MF) properties. SNRs are therefore observed with space and ground based observatories in the X-ray, γ -ray and radio bands, and modelled with advanced codes for magnetohydrodynamic (MHD) and/or particle kinetics.

The interstellar MF (ISMF) creates different obliquity angles with the shock normal in different places of the SNR surface. Efficiencies

of injection and acceleration, compression and/or amplification of ISMF may depend on the shock obliquity. Therefore, in order to model non-thermal emission, it is important to make assumptions about ISMF orientation around these objects.

In many cases, the ISMF, galactic in origin, may be assumed to be rather uniform on the scales of SNR sizes. This is likely to be the case of the bilateral SNRs (hereafter BSNRs; Kesteven & Caswell 1987; Gaensler 1998; but see Orlando et al. 2007, for implications of asymmetries in BSNRs), which are characterized by strong, opposite limbs. BSNRs with symmetric structure in radio images limit the orientation of the ISMF component in the plane of the sky. In the case of the BSNR archetype SN 1006, for instance, the ISMF may be parallel to the symmetry axis, spanning from south east (SE) to north west (NW), or be perpendicular to it, running from north east (NE)

*E-mail: petruk@lms.lviv.ua

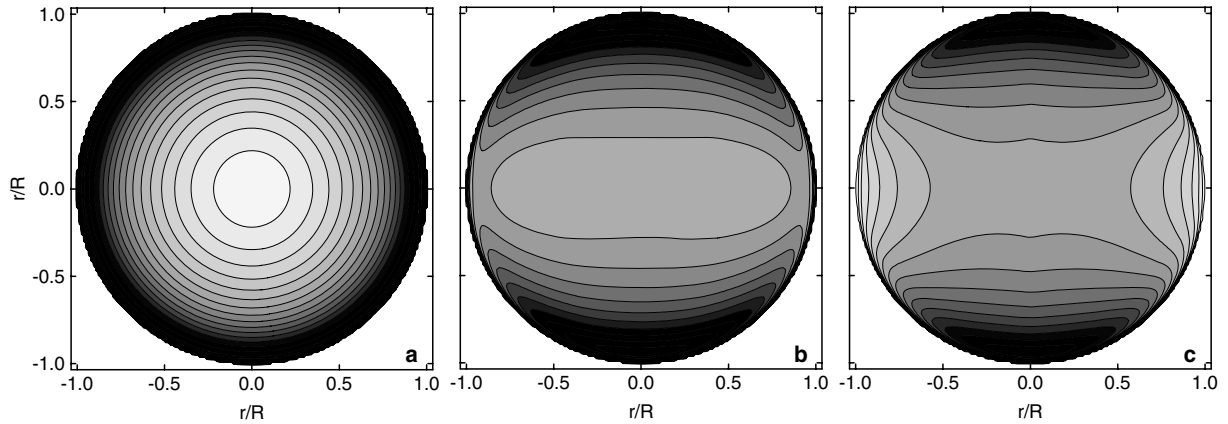


Figure 1. Surface brightness distributions (in linear scale) of the radio emission of adiabatic SNR for different aspect angles: $\phi_o = 0^\circ$ (a), 60° (b), 90° (c). Uniform ISM, uniform ISMF and isotropic injection are assumed. In cases (b) and (c), the component of ISMF in the plane of the sky is parallel to the horizontal axis. In all three plots, the levels of brightness are spaced in the same way.

to south west (SW). The former corresponds to barrel-like (equatorial belt) structure and the latter to polar-cap structure (Rothenflug et al. 2004). However, in order to draw reliable conclusions about the shock obliquity, it is also necessary to consider the aspect angle – the angle between ISMF and the line of sight – which is still unknown.

In the present paper, we propose a new method for determination of the aspect angle. We extract the azimuthal profiles of the synchrotron surface brightness distribution in a given SNR and compare the observed profiles with those synthesized from theoretical models, making different assumptions on the aspect angle and/or on the details of injection and acceleration of electrons. The ‘true’ aspect angle is that of the best-fitting model. As a first application of the method, we analysed SN 1006.

The plan of the paper is as follows. The method itself is explained in Section 2 where results of numerical simulations are presented. In Section 3, we use our method to determine the aspect angle towards SN 1006. To achieve this, we produced a new radio image of the remnant, obtained from re-analysis of archival Very Large Array (VLA) and Parkes data. An approximate formula for the azimuthal variation of the radio surface brightness is presented in Section 4 where we also discuss effects of the shock modification on our results as well as some consequences on the injection model in SN 1006.

2 ASPECT ANGLE IN BILATERAL SNRS: THE METHOD

The method to determine the aspect angle ϕ_o between ISMF and the line of sight on the basis of radio emission in SNRs can be deduced from the simulated radio maps produced for a Sedov SNR expanding through a uniform ISM and ISMF, presented in Fig. 1. As shown in the figure, the *azimuthal* profile of the surface brightness is sensitive to the aspect angle: it is constant for $\phi_o = 0^\circ$ [Fig. 1(a); ISMF is directed towards the observer] and it is steepest for $\phi_o = 90^\circ$ [Fig. 1(c); ISMF is in the plane of the sky]. Thus, comparison of an observed azimuthal profile with theoretical ones allows one to conclude about the aspect angle.

The radio surface brightness S at some ‘point’ of SNR image is

$$S \propto \int K B^{(s+1)/2} dl, \quad (1)$$

where s and K are the index and the normalization of the electron energy spectrum, respectively, B is the MF strength and the integration is along the line of sight within the volume of SNR. For a Sedov SNR in a uniform ISM and uniform ISMF, the downstream distributions of K and B are self-similar, i.e. may be written in the form $K = K_s(\Theta_o) \bar{K}(\bar{r})$, $B = B_s(\Theta_o) \bar{B}(\bar{r}, \Theta_o)$, where r is the radial distance from the centre of SNR, Θ_o is the shock obliquity angle between ISMF and the shock normal, index ‘s’ marks the immediate post-shock values and the upper bar marks the downstream variables normalized at their own values at the shock front (Reynolds 1998; Petruk 2006).

MF is generally a subject of compression, and under conditions of efficient cosmic ray acceleration, amplification on the shock. The MF can be expressed as $B_s = A_B(\Theta_o) B_o$ where A_B is a product of the compression factor σ_B and an amplification factor. Since it is unknown whether MF amplification depends on the shock obliquity, we assume it to be independent of Θ_o . In this case, the variation of the post-shock MF with obliquity is only determined by the compression (Reynolds 1998), $B_s \propto \sigma_B(\Theta_o) B_o$, where

$$\sigma_B(\Theta_o) = \left(\frac{1 + \sigma^2 \tan^2 \Theta_o}{1 + \tan^2 \Theta_o} \right)^{1/2}, \quad (2)$$

$\sigma = 4$ is the shock compression ratio for unmodified shocks (changes in this prescription and our results due to the shock modification are discussed in Section 4).

At the shock, the normalization, $K_s \propto \zeta(\Theta_o)$, where ζ is the injection efficiency defined as the fraction of accelerated electrons. There are three alternatives for dependence of injection efficiency ζ on obliquity of the shock typically considered in the literature: isotropic injection (i.e. ζ independent of Θ_o), quasi-parallel ($\zeta \propto \cos^2 \Theta_s$) or quasi-perpendicular ($\zeta \propto \sin^2 \Theta_s$) injection (Fulbright & Reynolds 1990). Therefore, the injection efficiency either decreases (quasi-parallel) or increases (quasi-perpendicular) with increasing obliquity or it is independent of Θ_o . The MF compression factor increases with Θ_o .

In symmetric, bilateral SNRs (like SN 1006¹), the possible orientations of the ISMF *in the plane of the sky* are limited. Namely,

¹ Note that SN 1006 is symmetric with respect to the axis between the two radio lobes. However, the lobes appear slanted and converging to the SE (see Orlando et al. 2007, for a possible explanation of this kind of asymmetry).

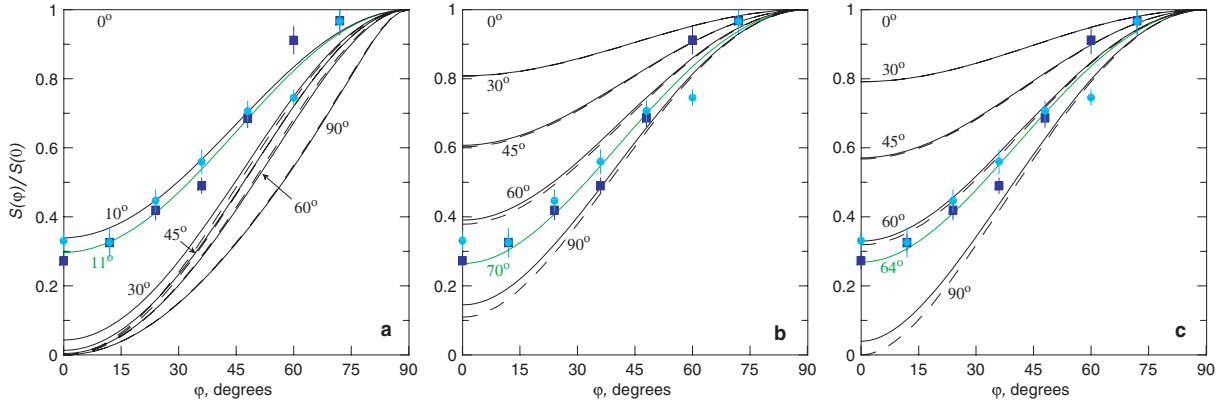


Figure 2. Azimuthal variation of the radio surface brightness $S(Q_{S_{\max}}, \varphi)$ for different aspect angles ϕ_0 . Numerical results (solid lines) are normalized to $S(Q_{S_{\max}}, \pi/2)$. Calculations are done for $b = 0$, $\beta = 0$, $s = 2.2$; the plots however are almost the same for different values of b , β and s . The models of injection are quasi-parallel (a), isotropic (b) and quasi-perpendicular (c). $\bar{\rho}_{S_{\max}} = 0.98$ (a) and $\bar{\rho}_{S_{\max}} = 0.97$ (b, c). Experimental data for SN 1006 are shown for region I (in blue) and II (in cyan). They are measured at 1.5 GHz between 12 and 14 arcmin from the centre and are normalized to the maximum value of 1σ errors. Azimuthal profiles given by the approximate formula (3) are shown by dashed lines.

ISMF may be parallel to the symmetry axis or perpendicular to it. For example, in SN 1006, if the injection is isotropic or quasi-perpendicular, the bright limbs correspond to the magnetic ‘equator’ (equatorial belt) and ISMF should be oriented in SE–NW direction. If injection prefers quasi-parallel shocks, the bright limbs of SN 1006 are two polar caps and MF should be oriented in the NE–SW direction. In other words, the model of injection determines the orientation of the plane-of-the-sky component of ISMF.

There are theoretical expectations that injection is higher at parallel shocks (Ellison et al. 1995; Völk, Berezhko & Ksenofontov 2003). In contrast, observational evidence seems to argue for isotropic or quasi-perpendicular injection in SNRs (Fulbright & Reynolds 1990; Orlando et al. 2007). We consider all three possibilities in this work.

We synthesized a number of radio surface brightness maps of a Sedov SNR evolving in a uniform ISM and uniform ISMF. We used the model of Reynolds (1998) with some extension presented in Petruk (2006). This model is able to account for the evolution of $K_s \propto V^{-b}$ and $A_B \propto V^{\beta/2}$, where b and β are constant and V is the shock velocity. These relations reflect an eventual evolution of the injection efficiency and MF amplification at the shock.

Radio maps of the model SNR were calculated for a range of indices: s from 2 to 2.2, b from $-3/2$ to 2, β from 0 to 2. For each set of parameters, we produced a series of images by changing the aspect angle ϕ_0 from 0 to $\pi/2$. For the image with $\phi_0 = \pi/2$ in each series, we found the radius of projection $Q_{S_{\max}}$ which corresponds to the position of the maximum brightness $S_{\max} = S(Q_{S_{\max}}, \varphi_{S_{\max}})$ (by definition $\varphi_{S_{\max}} = \pi/2$ for this position).² We then traced the surface brightness $S(Q_{S_{\max}}, \varphi)$ at this $Q_{S_{\max}}$ for azimuthal angles φ from 0 to $\pi/2$ and plotted these distributions normalized by the brightness $S(Q_{S_{\max}}, \varphi_{S_{\max}})$.

Fig. 2 shows the plots for different aspect angles, assuming $b = 0$, $\beta = 0$, $s = 2.2$, and considering the three models for obliquity dependence of injection efficiency. We found a reasonable result, namely that all the azimuthal profiles of surface brightness which

we obtained are almost insensitive (within 10–20 per cent) to the values of s , b and β (at least in the case of uniform ISM and uniform ISMF assumed here). That means the azimuthal profiles of radio brightness are almost independent of the shapes of the distributions of relativistic electrons and MF downstream of the shock. Such stability allows one to safely use the method proposed here for determination of the aspect angles from radio maps of SNRs if the ISM and ISMF in which SNR expands can be considered to be mostly uniform.

3 THE ASPECT ANGLE IN SN 1006

The method is applicable to SNRs expanding in almost uniform ISM and ISMF. BSNRs, particularly SN 1006, are ideal candidate targets of this study. In this SNR, uniform conditions are likely to be achievable since SN 1006 is located over 500 pc above the galactic plane. In addition, the SE edge of the SNR exhibits a near-spherical shape, a good argument for expansion of the shock into a uniform ISM.

3.1 Radio data

We now apply our method for the determination of the aspect angle to SN 1006 considerably the best example of a symmetric, bilateral SNR. To this end, we produced a new radio image of SN 1006 at $\lambda \sim 20$ cm.

This image was produced on the basis of archival VLA³ data obtained in 1991 October, 1992 February and 1992 July in the hybrid AnB, BnC and CnD configurations, respectively. The observations in the AnB configuration were carried out at 1370 and 1376 MHz, while the observations in the BnC and CnD arrays were performed at 1370 and 1665 MHz. The data corresponding to the more compact configurations of the VLA, BnC and CnD, were published as a part of an expansion study of SN 1006 (Moffett, Goss & Reynolds 1993), but not the data from the AnB configuration, which provides

² The radius $Q_{S_{\max}}$ is almost the same for any aspect angle, except for $\phi_0 < 30^\circ$ in the quasi-parallel model. In the case of quasi-parallel injection, the angle $\phi_0 = 30^\circ$ roughly separates cases with a centrally peaked morphology ($\phi_0 < 30^\circ$) and a bilateral one ($\phi_0 > 30^\circ$).

³ The VLA of the National Radio Astronomy Observatory is a facility of the National Science Foundation operated under cooperative agreement by Associated Universities, Inc.

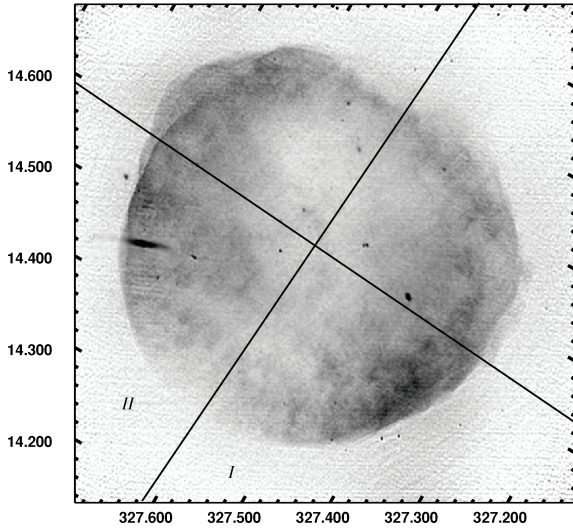


Figure 3. Radio image of SN 1006, in linear scale (galactic coordinates). Axes outline regions I and II used in our analysis.

the highest angular resolution of southern sources. The new interferometric image is produced on the basis of 4 h per configuration (the maximum possible taking into account the elevation restrictions for this source when observed from the northern hemisphere) and recovers emission from all spatial structures with angular scales between a few arcsec and 15 arcmin.

All data were processed using the MYRIAD software package. To avoid the diffraction effects produced by point sources present in the field, for each of the brightest sources we imaged a small region around, and the clean components were Fourier transformed and subtracted from the visibilities. The residual visibilities, containing all the source structure except for the offending point sources were then imaged and the point sources were added back into the SN 1006 image in the image plane. To recover flux density contribution from structures on angular scales larger than 15 arcmin (which is important in this case since SN 1006 is ~ 30 arcmin in diameter) we added single dish observations acquired in 2002 with the Parkes 64 m radiotelescope placed in Australia. Also, since the primary beam of the VLA (the half-power beamwidth of a single VLA antenna) at $\lambda 20$ cm is 32 arcmin, comparable to the size of the source, a correction was applied to the interferometric data taking into account the attenuation introduced near the primary beam edge.

The final image has a synthesized beam of 7.7×4.8 arcsec², position angle $8^\circ.3$, and an rms noise of 1×10^{-4} Jy beam⁻¹. When combined with Parkes single-dish data, the total recovered flux is $S = 14.9$ Jy, in excellent agreement with previous estimates from Green's (2006) catalogue of SNRs.⁴ The new image is presented in Fig. 3. The accuracy of the field point sources serves for comparison to appreciate the quality of the new image that resolves the SNR radio features down to the same fine spatial resolution.⁵

⁴ <http://mrao.cam.ac.uk/snrs/>

⁵ After submission of our paper, a new radio image of SN 1006 has been reported by Cassam-Chenaï et al. (2008). This image, based on new observations, has an angular resolution of $\sim 6 \times 9$ arcsec², comparable to that achieved in this work. It has a better noise level ($20 \mu\text{Jy beam}^{-1}$); however, it lacks the large spatial scale structures that were recovered in our image with the addition of single dish data.

3.2 Results

To determine the MF orientation, we only considered the SE half of SN1006 (regions I and II in Fig. 3) because this part is quite spherical and therefore is more appropriate for comparison with the numerical results obtained in Section 2 for a SNR in uniform ISM. From the radio map of SN 1006, we extracted the radial brightness profiles (along radii of the SNR projection separated on $\Delta\varphi = 12^\circ$). The experimental radial distributions are subject to pixel-to-pixel variations. In order to lower the possibility of error due to fluctuations in observational data, we calculated the averages of brightness and 1σ errors within 12 to 14 arcmin from the centre of SN 1006 (where the maximum in radial distribution of the surface brightness is located).

Experimental data are compared with the theoretical results in Fig. 2. The estimated aspect angle ϕ_o differs much for the polar-cap and the equatorial-rim models of SN 1006. From the numerical simulations, the best-fitting aspect angle is $\phi_o = 70^\circ \pm 4.2^\circ$ for isotropic injection, $\phi_o = 64^\circ \pm 2.8^\circ$ for quasi-perpendicular injection and $\phi_o = 11^\circ \pm 0.8^\circ$ for quasi-parallel injection. Considering an isotropic injection and equatorial-rim model for SN 1006, Reynolds (1996) found a similar aspect angle, $\phi_o = 60^\circ$.

4 DISCUSSION

4.1 Basic processes determining the azimuthal brightness profiles

We found that the azimuthal profiles of the radio surface brightness of the Sedov SNR are almost independent of the shapes of the distributions of relativistic electrons and MF downstream of the shock. Close to the shock, the azimuthal variations of the radio brightness of the SNR may therefore be approximately described as (Appendix A):

$$S_\ell(\varphi) \propto \zeta [\Theta_{o,\text{eff}}(\varphi, \phi_o)] A_B [\Theta_{o,\text{eff}}(\varphi, \phi_o)]^{(s+1)/2}, \quad (3)$$

where

$$\cos \Theta_{o,\text{eff}} = \cos \varphi \sin \phi_o, \quad (4)$$

for isotropic or quasi-perpendicular injection and

$$\cos \Theta_{o,\text{eff}} = \sin \varphi \sin \phi_o, \quad (5)$$

for quasi-parallel injections. (Equation 3 is not valid for a centrally brightened SNR.)

In order to compare the approximate azimuthal profiles given by this formula with the numerical results, we plotted them in Fig. 2 with dashed lines. This figure shows that (3) can be used as an approximation for the azimuthal distributions of the radio surface brightness in SNRs evolving in uniform medium and uniform MF.

An important consequence of (3) is that there are *two basic processes* which determine the *azimuthal* distribution of the radio surface brightness in SNR evolving in uniform ISM and uniform ISMF: electron injection and compression (and/or amplification) of ISMF on the shock.

4.2 Modified shock

The estimations in Section 3.2 were obtained for a shock compression ratio $\sigma = 4$. Modified shocks may be responsible for larger compression, $\sigma = 7$. Modelling the situation out of the Bohm limit, we may use such compression factor together with (2). Essentially, the estimated aspect angle does not change in this case. Namely, it becomes $\phi_o = 65^\circ \pm 4.2^\circ$, $64^\circ \pm 2.8^\circ$ and $11^\circ \pm 0.8^\circ$ for isotropic,

quasi-perpendicular and quasi-parallel injection, respectively. Thus, even if the shock is modified but not in the Bohm limit, the estimation for the aspect angle obtained under the assumption of an unmodified shock, may well be valid.

Our model is based on a classical MHD approach where the parallel and perpendicular components of the ambient MF are compressed in different ways, as it is given by (2) [e.g. Korobeinikov & Karlikov (1960) or Korobeinikov (1991, chapter 7.4) for the self-similar solution of the problem of the strong point explosion in a constant MF]. This approach might not be valid in a limit in which the turbulent MF dominates, as in the case of the very efficient non-linear particle acceleration consistent with Bohm diffusion. The quasi-parallel theory assumes in this case that the turbulence is produced ahead of the shock, not downstream. The compression of the (already turbulent) MF then does not depend on the original obliquity (Berezhko, Ksenofontov & Völk 2002; Völk et al. 2003). Rakowski, Laming & Ghavamian (2008) argue that shocks of different initial obliquity subject to MF amplification become perpendicular immediately upstream. We may model such situation assuming $\sigma_B(\theta_o)$ is a constant instead of using (2) and $\bar{B}(\bar{r}, \Theta_o) = \bar{B}(\bar{r}, \pi/2)$.

The estimations of the aspect angle in this case are $58^\circ \pm 2.8^\circ$ and $11^\circ \pm 0.9^\circ$ for quasi-perpendicular and quasi-parallel injection, respectively. Isotropic injection produces constant azimuthal profiles in this case, i.e. the modelled SNR looks like a rim for any aspect angle.

The estimated aspect angles in the assumption of the Bohm limit are close to those obtained for an unmodified shock, except for the isotropic injection. Isotropic injection, together with the assumption that the downstream MF is independent of obliquity is not able to reproduce bilateral morphology of SNR. There is no azimuthal variation of the radio surface brightness in this case, in agreement with (3).

4.3 Injection efficiency and obliquity

It is worth emphasizing that our analysis may have some implications for the model of injection efficiency.

Our argument against the quasi-parallel injection is the morphology of SN 1006, it should have in uniform ISM and uniform ISMF. Fig. 4 shows an image of SN 1006 in case of the quasi-parallel injection ($\zeta \propto \cos^2 \Theta_s$) and aspect angle $\phi_o = 11^\circ$. Since the ambient MF should be almost aligned with the line of sight and injections prefer parallel shocks ('polar caps' directed towards and away from observer), the brightness distribution of SN 1006 should be centrally brightened (with one or two radio 'eyes' within thermal X-ray rim), contrary to what is observed.

Our argument seems therefore to disagree with polar-cap morphology, and favours a NW–SE orientation of ISMF around this SNR.

Rothenflug et al. (2004) suggested a criterion, which is considered as an argument on behalf of the polar-cap model for SN 1006. Namely, if SN 1006 has an equatorial rim the observer should see some emission between the bright limbs. Numerically, the value of the parameter $R_{\pi/3}$ defined as a ratio between total power coming from the interior and that from the limbs should be $R_{\pi/3} > 0.5$ if SN 1006 is a barrel. The most likely explanation for the smaller value of $R_{\pi/3}$ is that the visible limbs are polar caps (Rothenflug et al. 2004). The value of this ratio is $R_{\pi/3} \approx 0.7$ in radio (Rothenflug et al. 2004). Therefore, based on the $R_{\pi/3}$ criterion alone, the radio data itself cannot give preference neither to equatorial-rim nor to polar-cap model of SN 1006. However, $R_{\pi/3} \leq 0.3$ in X-rays (Rothenflug et al. 2004), preferring therefore the latter model.

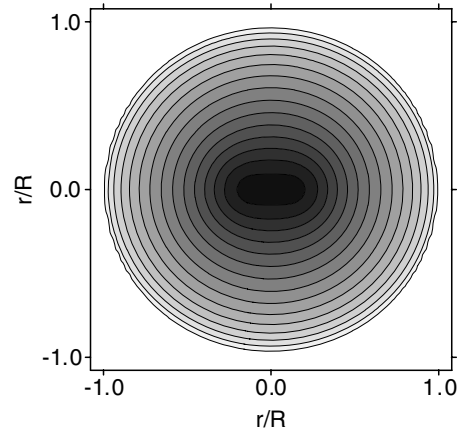


Figure 4. Surface brightness distribution (in linear scale) of SNR with the same parameters as in Fig. 2. The surface brightness distribution is calculated assuming the quasi-parallel model of injection and the aspect angle $\phi_o = 11^\circ$. The component of ISMF in the plane of the sky is parallel to the horizontal axis. The levels of brightness are spaced in the same way as on the Fig 1.

To this end, our argument against polar caps is in contradiction with $R_{\pi/3}$ criterion applied to X-ray data. Note that the $R_{\pi/3}$ criterion is obtained for cylindrical source of isotropic emission. It would be interesting to see how deviations from these assumptions may affect the criterion. Our models assume a uniform ISM and uniform ISMF. Could it be possible to reproduce the bilateral morphology (i.e. to obtain $\phi_o > 30^\circ$) with quasi-parallel injection if one considers a gradient in the ISMF? Assuming the contrast of the ISMF between the NE and SE regions can be determined by the relationship $B_{SE}/B_{NE} \simeq (S_{SE}/S_{NE})^{2/3}$, a ratio of 4 for $\phi_o = 45^\circ$, and 20 for 60° , could make the azimuthal profile of radio emission comparable to the observed one. Further investigation, including multidimensional modelling of SN 1006, as recent very-high energy (VHE) γ -ray data could help us to understand the nature of morphology of this SNR.

5 CONCLUSIONS

Radio images of SNRs can be a useful probe to determine the orientation of ISMF around SNRs. We develop a method for determination of the aspect angle between ISMF and the line of sight, through the comparison between radio observations and model calculations. It is based on a property of azimuthal variation of radio surface brightness. Namely, the azimuthal profile is almost insensitive to the downstream evolution of MF and relativistic electrons. In contrast, it is sensitive to the obliquity dependences of both the injection efficiency and the compression (amplification) factor of ISMF. The obliquity angle, the azimuthal angle and the aspect angle are geometrically related. The simple expression (3) together with certain assumptions about the model of injection [where isotropic or quasi-perpendicular injection appears to be suggested by a number of arguments (Fulbright & Reynolds 1990)] may be used in order to fit the observed azimuthal profile and to approximately estimate the aspect angle.

We applied our method to determine the aspect angle in SN 1006. A new radio image of SN 1006 obtained from archival VLA and Parkes data is reported. The image has very good angular resolution and has contributions from all spatial scales recovered. The use of the numerical modelling together with the new observations reported here allows us to find the best-fitting value of the aspect

angle in case of unmodified shock: $\phi_o = 70^\circ \pm 4.2^\circ$ for the case of isotropic injection, $\phi_o = 64^\circ \pm 2.8^\circ$ for quasi-perpendicular injection (equatorial-belt model of SNR in both cases) and $\phi_o = 11^\circ \pm 0.8^\circ$ for quasi-parallel injection (polar-cap model). The angles estimated under assumption of modified shock are quite close to those given above.

There are some limitations from our results on the model of injection. In quasi-parallel and quasi-perpendicular models, aspect angles are expected (and found) to be similar in both modified and unmodified shocks because the obliquity variation of injection dominates the obliquity variation of ISMF compression/amplification. Rather flat observed azimuthal radio profile strongly prefers $\phi_o < 30^\circ$ if injection is assumed quasi-parallel [Fig. 2(a)], that is for polar-cap model of SN 1006. In this case, SN 1006 should be centrally brightened, contrary to what is observed. Next, if one assumes the shock in SN1006 is so strongly modified that compression of ISMF is independent of obliquity (Bohm limit), then the only possible injection model is quasi-perpendicular, because isotropic injection and constant A_B results in constant azimuthal profiles of the radio surface brightness, again contrary to what is observed.

Rejection of the quasi-parallel injection model in SN 1006 means that the initial ISMF is directed from SE to NW and SN 1006 has a barrel-shaped, rather than polar-cap, morphology.

With our results, we come to a puzzling issue which should be investigated in the future: Rothenflug et al. (2004) $R_{\pi/3}$ criterion applied to the X-ray emission seems to exclude the equatorial model of SN 1006 while the analysis of the azimuthal radio profiles seems to be against of the polar-cap scenario.

ACKNOWLEDGMENTS

The draft of the paper was improved thanks to critical remarks of anonymous referee. FB, MM, and SO acknowledge Consorzio COMETA under the PI2S2 Project, a project co-funded by the Italian Ministry of University and Research (MIUR) within the Piano Operativo Nazionale ‘Ricerca Scientifica, Sviluppo Tecnologico, Alta Formazione’ (PON 2000–2006). OP and DI acknowledge the program ‘Kosmomikrofizyka’ of National Academy of Sciences (Ukraine). GD and GC are members of CIC-CONICET (Argentina) and acknowledge support of PIP-CONICET 6433. DI acknowledges the support from the INTAS project No. 05-1000008-7865. IT acknowledges the support from the INTAS YSF grant No. 06-1000014-6348.

REFERENCES

- Berezhko E., Ksenofontov L., Völk H., 2002, A&A, 395, 943
 Cassam-Chenaï G., Hughes J. P., Reynoso E. M., Badenes C., Moffett D., 2008, ApJ, 680, 1180
 Ellison D., Baring M., Jones F., 1995, ApJ, 453, 873
 Fulbright M. S., Reynolds S. P., 1990, ApJ, 357, 591,
 Gaensler B. M., 1998, ApJ, 493, 781
 Kesteven M. J., Caswell J. L., 1987, A&A, 183, 118
 Korobeinikov V., 1991, Problems of Point Blast Theory. Springer-Verlag, New York, p. 400
 Korobeinikov V., Karlikov V., 1960, DoSSR (Doklady Akademii Nauk SSSR), 133, 764
 Moffett D. A., Goss W. M., Reynolds S. P., 1993, AJ, 106, 1566
 Orlando S., Bocchino F., Reale F., Peres G., Petruk O., 2007, A&A, 470, 927,
 Petruk O., 2006, A&A, 460, 375
 Rakowski C., Laming J., Ghavamian P., 2008, ApJ, 684, 348

- Reynolds S. P., 1996, ApJ, 459, L13
 Reynolds S. P., 1998, ApJ, 493, 375
 Rothenflug R., Ballet J., Dubner G., Giacani E., Decourchelle A., Ferrando P., 2004, A&A, 425, 121
 Völk H., Berezhko E., Ksenofontov L., 2003, A&A, 409, 563

APPENDIX A: APPROXIMATE FORMULA FOR AZIMUTHAL VARIATION OF THE RADIO SURFACE BRIGHTNESS IN SEDOV SNR

Here, we derive an approximate formula for azimuthal variation of the radio surface brightness. This formula allows one to avoid detailed numerical simulations and may be useful in situations where the approximate estimation of the aspect angle is reasonable. In addition, the formula allows us to have deeper insight in the main factors determining the azimuthal variation of the radio surface brightness in SNRs.

The downstream distributions of K and B in a Sedov SNR in uniform ISM and uniform ISMF are

$$K \propto \zeta(\Theta_o) \bar{K}(\bar{r}), \quad B \propto A_B(\Theta_o) \bar{B}(\bar{r}, \Theta_o). \quad (A1)$$

If one neglects the small differences in downstream distributions of the parallel and perpendicular components of B (Fig. 1 Reynolds 1998), then

$$\bar{B}(\bar{r}, \Theta_o) \approx \bar{B}(\bar{r}). \quad (A2)$$

The obliquity angle Θ_o is different for each radial sector of 3D object. It is determined, for any position within SNR, by the set $(\varphi, \bar{r}/\varrho, \phi_o)$. Integration along the line of sight gathers information from different radial sectors, with different obliquities. Let us determine the ‘effective’ obliquity angle by the relation

$$\Theta_{o,\text{eff}}(\varphi, \phi_o) = \Theta_o(\varphi, 1, \phi_o). \quad (A3)$$

Actually, $\Theta_{o,\text{eff}}$ for a given azimuth equals to the obliquity angle for a sector with the same azimuth lying in the plane of the sky (i.e. in the plane being perpendicular to the line of sight and containing the centre of SNR). Θ_o varies around $\Theta_{o,\text{eff}}$ during integration along the line of sight. The closer ϱ to the edge of SNR projection the smaller the range for variation of Θ_o and more accurate is our approximation. (Actually, we used ϱ corresponding to maximum in radial brightness distribution which happens rather close to the shock.)

Let us consider the azimuthal profile of the radio brightness S_ϱ at a given radius ϱ from the centre of the SNR projection.

With the use of $\Theta_{o,\text{eff}}$, the azimuthal variation of the radio brightness for fixed ϱ may approximately be written from (1) as

$$S_\varrho \propto \zeta(\Theta_{o,\text{eff}}) A_B(\Theta_{o,\text{eff}})^{(s+1)/2} \int_{\bar{q}}^1 \frac{\bar{K}(\bar{r}) \bar{B}(\bar{r})^{(s+1)/2} \bar{r} d\bar{r}}{\sqrt{\bar{r}^2 - \bar{q}^2}}. \quad (A4)$$

The integral in (A4) is the same for any azimuthal angle φ . The azimuthal variation of the radio brightness is therefore approximately determined by

$$S_\varrho(\varphi) \propto \zeta \left[\Theta_{o,\text{eff}}(\varphi, \phi_o) \right] A_B \left[\Theta_{o,\text{eff}}(\varphi, \phi_o) \right]^{(s+1)/2}. \quad (A5)$$

The relation between the azimuthal angle φ , the obliquity angle $\Theta_{o,\text{eff}}$ and the aspect angle ϕ_o is as simple as

$$\cos \Theta_{o,\text{eff}} = \cos \varphi \sin \phi_o, \quad (A6)$$

for assumption of isotropic or quasi-perpendicular injection

$$\cos \Theta_{o,\text{eff}} = \sin \varphi \sin \phi_o, \quad (A7)$$

for quasi-parallel injections (the relations are different because we define the azimuth angle $\varphi_{\text{Smax}} = \pi/2$ at the position of the maximum brightness).

The accuracy of the approximation (A5) is shown in Fig. 2. The azimuthal profiles is sensitive to ϱ in quasi-parallel case for aspect angles less than about 30° , i.e. for SNR with centrally brightened radio morphology ($\zeta \propto \cos^2\Theta_0$ and, for small aspect

angles, $\Theta_0 \rightarrow \pi/2$ on the periphery of SNR and thus $\zeta \rightarrow 0$ there). Therefore, the formula (A5) does not give correct profiles in the case of quasi-parallel injection for $\phi_0 < 30^\circ$, unless $\bar{\varrho} \rightarrow 1$.

This paper has been typeset from a $\text{\TeX}/\text{\LaTeX}$ file prepared by the author.